An experimental study of sand boiling in relation to shearing characteristics of liquefied soil

Une étude expérimentale du sable bouillant en fonction des caractéristiques de cisaillement du sol liquéfié

Tadashi Kawai, Jongkwan Kim, Motoki Kazama, Takumi Yoshii

Dept. of Civil Engineering, Tohoku University, Japan, tadashi.kawai.b2@tohoku.ac.jp

ABSTRACT: Ground settlements after liquefaction are usually evaluated based on the amount of soil contraction caused by shearing, the so-called negative dilatancy. It means that during and after an earthquake, a kind of consolidation occurs and a large percentage of the erupted material tends to be water. As such the soil particles erupted by sand boiling are usually ignored when estimating the amount of the settlement. In some special case, however, there is so much erupted soil that it cannot be ignored when evaluating ground settlement. This was the case in the liquefactions in Urayasu city during the 2011 Tohoku great earthquake and in Christchurch city during the 2011 Christchurch earthquake. In this paper, a series of shearing tests using a small shearing box were conducted to cause sand boiling using various shear strain histories and different kinds of materials. The results showed that in soils with low permeability, the amount of erupted soil is related to the critical shear strain, which is the strain required to for the recovery of the effective stress after liquefaction. It was also shown that the amount of ground settlement increases with increases in the critical strain.

RÉSUMÉ : Les tassements du sol qui se produisent après sa liquéfaction sont généralement évalués en fonction de la contraction du sol causée par le cisaillement et qui s'appelle la dilatance négative. Cela signifie que pendant et après l'événement d'un tremblement de terre, une sorte de consolidation se produit et il est estimé que la partie principale des matériaux éclatés devrait être de l'eau. Ainsi, les particules de sol éclatées par l'ébullition de sable sont généralement ignorées pour estimer la quantité du tassement. En revanche, dans certains cas, comme les liquéfactions qui se sont produits à la ville d'Urayasu pendant le grand tremblement de terre de Tohoku en 2011 ainsi que dans la ville de Christchurch lors du séisme de Christchurch en 2011, les quantités des sols éclatés étaient trop significatives pour être ignorées dans l'évaluation des tassements du sol. Dans cet article, une série des tests de cisaillement à l'aide d'une petite boîte de cisaillement ont été réalisés pour provoquer le sable à bouillir en changeant les historiques des déformations de cisaillement ainsi que les types des matériaux utilisés. Les résultats montrent que les quantités des sols éclatées sont liées à la contrainte de cisaillement critique, qui est la déformation nécessaire pour provoquer la récupération de la contrainte effective après la liquéfaction, si la perméabilité du sol était faible. En outre, il est indiqué que plus la déformation critique devient grande, plus du tassement du sol se produit.

KEYWORDS: Liquefaction, boiling sand, settlement, critical shear strain

1 INTRODUCTION

Measurements of negative dilatancy, which is the amount of soil contraction caused by shearing, are typically taken to determine the extent of the ground settlements after liquefaction (e.g. Ishihara and Yoshimine 1992). This can be understood in that the erupted material after an earthquake is expected to be largely made up of water. As such, the soil particles erupted by the sand boiling tend to be ignored when the amount of the settlement is estimated. Liquefactions in some special cases, however, like that in Urayasu city during the 2011 Tohoku great earthquake and in Christchurch city during the 2011 Christchurch earthquake, present a different scenario. In such cases, there was so much erupted soil that it was not possible to ignore it when evaluating the extent of the ground settlement. The difference between thse cases is shown in Figure 1: Type A is the type of sand boiling usually observed after liquefaction, and Type B sand boiling is the type observed in Urayasu and Christchurch. Type B sand boiling occurs due to the squeezing of the liquefied soft soil under the weight of the upper ground and structures. The differences between these two types of sand boiling are many.

Type A sand boiling is more common, and is caused by the consolidation of the soil skeleton, which is potentially contracted by shearing during the earthquake, the so-called negative dilatancy under undrained conditions. Since the soil skeleton in all parts of the liquefied layer drains the pore water, the huge volume of erupted water furiously erodes the soil skeleton near the pathway. This happens in all the sand layers, able to contract by shearing and moderate permeability. On the contrary, if permeability becomes lower and the shear modulus

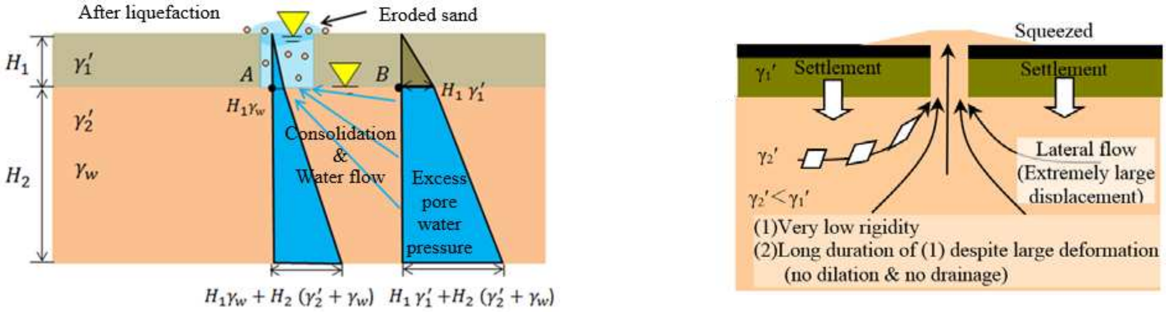

(a)Type A: Ordinary shrinkage of the soil skeleton and consolidation.

(b)Type B: Squeezing of the total volume (target of this investigation).

Figure 1. Schematic illustrations of the two expected mechanisms of the boiling sand.

remains extremely small even after large deformation, a large amount of shearing occurs and the soil skeleton is squeezed out through the defects in the upper soil layer before the effective stress and the rigidity of the soil skeleton is recovered by drainage.

In order to confirm the probability of the occurrence of Type B sand boiling, a series of model tests were conducted using a small shearing box to cause the sand boiling. A variety of materials, each with different contraction potentials due to shearing and different permeabilities, were sheared to create different shear strain histories and to cause liquefaction.

2 MATERIALS

In order to confirm the occurrence of Type B sand boiling, a variety of different sands were prepared, including sand collected in Urayasu city and mixed sands with different fines contents, as shown in Figure 2. The mixed sands were composed of a silica sand named Keisa and a quartz fine was used for Q50, Q30 and Q10. The silica sand, which had a maximum diameter of less than 0.4mm was mixed with 50%, 30% and 10% of the quartz fine as a percentage of the total weight, respectively. The MX sample was composed of a silica sand with maximum diameter of less than 0.8mm and 60% quartz fine. The MX sample was well graded compared to the Q-series sample.

As mentioned above, it is largely assumed that Type B sand boiling happens only in conditions with low permeability and large shear deformation without the recovery of rigidity (no dilation of the soil skeleton), so the addition of such large percentages of fines (up to 60%) was intended to such conditions to various extents. The physical properties of those samples are shown in Table 1.

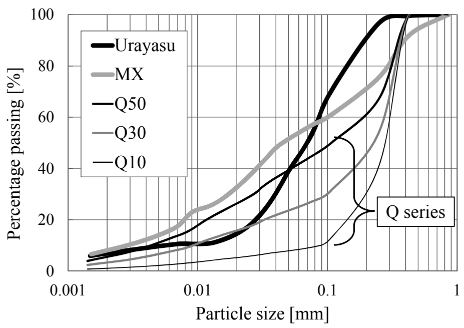

Figure 2. Particle size distribution curves of the tested materials.

Table 1. Physical properties of the tested materials.

	Urayasu	*MX*	*Q50*	*Q30*	*Q10*
Gs	2.62	2.74	2.72	2.73	2.74
e_{max}	1.62	1.59	1.37	1.20	1.02
e_{min}	0.88	0.60	0.55	0.46	0.52

3 SHEAR BOX TESTS

3 .1 *Testing method*

Figure 3 shows a schematic cross-section of the test apparatus. The material was poured into a shear box, with the following dimensions: L100mm x W100mm x B100mm. So that liquefaction would easily occur, the sample was packed as loosely as possible. Then dead weight was set in place to consolidate the sample up to a vertical pressure of 9.5kPa. A pipe 13mm in diameter and 120mm in height was set at the center of the top plate of the shear box, and the other part of the top surface was covered by a rubber membrane so that sand boiling would occur only through the stand pipe. During consolidation, a plastic rod with almost the same diameter as that of the inner diameter of the pipe was used as a plug to avoid the pipe being filled with the squeezed material before liquefaction process.

Since the purpose of this paper is only to confirm the occurrence of the type B sand boiling, these conditions, e.g. the overburden pressure and the size of stand pipe, were determined only by the limitations of the apparatus and were not related to any concrete in-situ image.

After the consolidation process was completed, the sample was sheared by the horizontal movement of the bottom plate, which was connected to a motor as shown in Figure 3. In some cases, instead of shearing, liquefaction was caused by tapping with a hammer to investigate the influence of the magnitude of shear deformation on the amount of erupted sand. The test conditions and some of the results are summaraized in Table 2.

Typical time histories of the relative displacements between the top plate and the bottom plate for both shearing and tapping are shown in Figure 4. Once it had been confirmed that liquefaction occured when the excess pore pressure ratio had reached approximately unity, the shearing process was ceased and the plug was pulled out to allow the material which had accumulated inside the standing pipe (if any) to flow out.

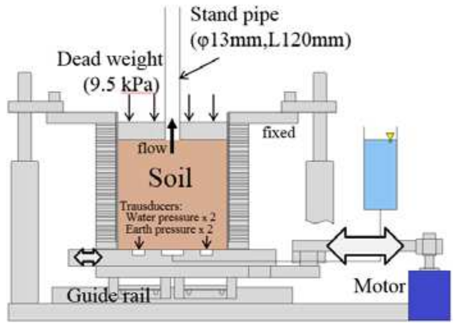

Figure 3. Cross section of the test apparatus.

Table 2. Test cases and the conditions.

Case	Material	Liq. method	Max. E.W.P.R	Void ratio before liq.	Erupted volume
#1	Urayasu	Shear	1.0	1.18	18.5
#2		Shear	1.0	1.28	21.6
#3	MX	Shear	0.93	0.51	39.0
#4		Shear	1.0	0.53	32.5
#5		Tap	0.82	0.55	17.8
#6	Q50	Shear	0.97	0.54	27.9
#7		Tap	0.84	0.59	2.9
#8	Q30	Shear	0.96	0.59	8.5
#9	Q10	Shear	1.0	0.80	8.1

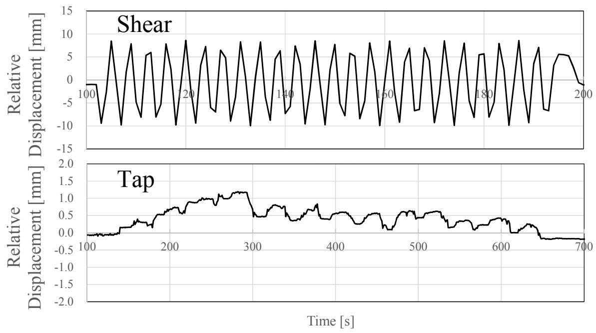

Figure 4. Typical time histories of the lateral displacements and the pore water pressure ratios.

In Figure 5, typical time histories of the excess water pressure ratio (E.W.P.R.), which were calculated using the records from the water pressure transducer on the bottom plate, are shown. Although the E.W.P.R. started to drop just after the shearing process ceased in all the cases, the starting time and duration of sand boiling were different in each case. This was due not only material properties like permeability, potential of contraction and shear modulus, but other conditions including the dimensions of the box and the pipe, the depth, the shape and the locations of the liquefied layer, and so on.

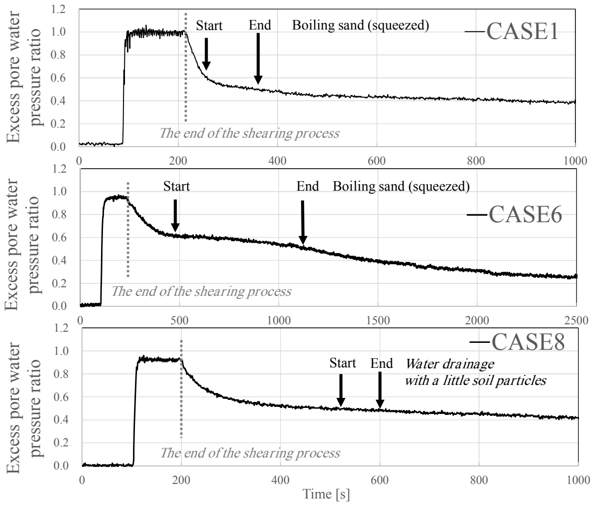

Figure 5. Typical time histories of the lateral displacements and the pore water pressure ratios.

3.2 *Results*

The amounts of erupted soil shown in Table 2 are plotted in Figure 6. Since the apparatus used was very simple and quite rough, some test cases were repeated to confirm the reproducibility of the phenomenon. A comparison of the results between CASE1 and CASE2, and also between CASE3 and CASE4 indicates that the difference observed in the tests conducted under the similar conditions was small.

Among the materials tested here, the MX sample was the most vulnerable to being squeezed, with Type B sand boiling taking place, as shown in Figure 7. The colored sand was recognizable as lines even after sand boiling and it indicated that the liquefied sand was highly sheared instead of random flowing. Although this in itself was sufficient to illustrate the rough movements of the sand layer, clearly three dimensional data was required to evaluate the strains quantitatively. This cross-section was parallel to the direction of the one dimensional lateral shearing and while large disturbances were apparent in the region close to both ends, totally different colored sand patterns were observed if the cross-section perpendicular to the shearing direction was chosen.

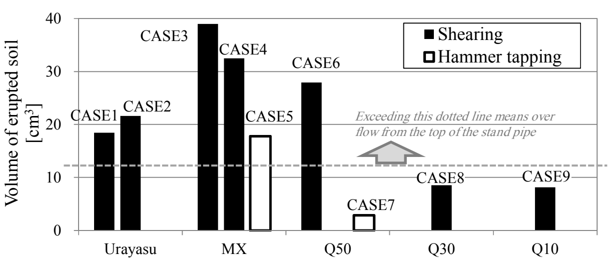

Figure 6. Erupted volumes through the stand pipe (φ=13mm, L=120mm).

In general, a larger amount of fines resulted in smaller permeability. The Q-series materials were prepared to investigate the influence of permeabilities. As shown in Figure 8 (CASE8), the permeability of Q30 was sufficient to result in the disgregation of the soil particles and water.

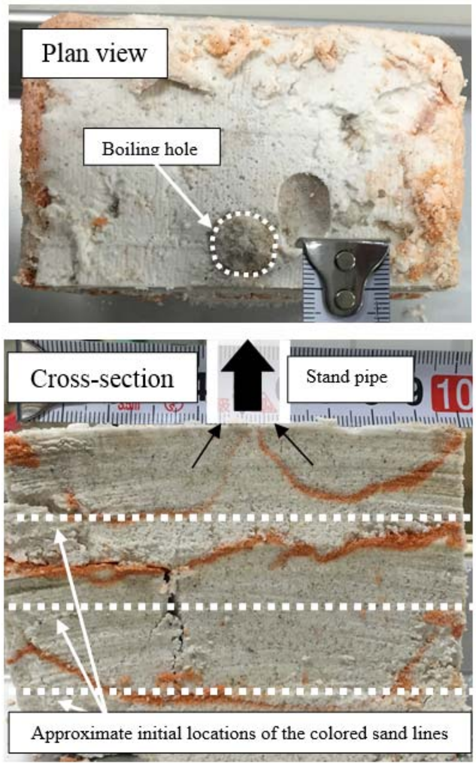

Figure 7. The movements of the colored sand after sand boiling in the MX sand specimen.

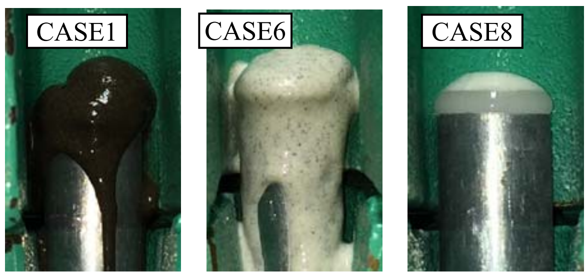

Figure 8. Typical boiling sand results.

4 DISCUSSIONS

While all the samples in this investigation were prepared at their loosest possible state, the resultant void ratios were scattered, as shown in Table 2. From the void ratio point of view, the Urayasu sample was more contractive and then erupted the largest amount of sand boiling among all the materials tested here. In spite of the smaller void ratio, which means denser state, the amounts of MX sample and Q50 sample were larger than Urayasu sample. It should be added that the critical shear strain (Yasuda et al. 1999), explained in Figure 9, might be more directly related to the amount of the type B sand boiling than the contraction potential represented by the void ratio. That is, since the observed deformation shown in Figure 7 suggests an extremely large amount of shear deformation was needed to cause Type B sand boiling, most important indicator would be whether the dilation of the sheared sample was small enough for the sample to remain under the tiny shear modulus condition.

Consider a liquefied soil element in the rather wide area to remain small rigidity, which means small effective stress, even after being highly sheared, the presumable causes are that the soil in itself is too contractive to recover effective stress even after largely deformed, as shown in Figure 9, and/or that the surrounding elements supply sufficient water to interfere the element to recover the effective stress. As shown in Figure 10 (Kim et al. 2015), the critical shear strain is closely related to the ultimate volumetric strain, the large value of which indicate that the soil is highly contractive. Therefore, from the point of view of the above two causes, the critical shear strain should be a better identifier of the amount of Type B sand boiling.

Although the minimum void ratio was required, the JGS standard cannot be applied to samples with a fines content of over 5%. Kim obtained the minimum void ratios, denoted by $e_{min,c}$, by a series of cyclic shear and consolidation steps, as shown in Table 3. Using those values, the critical shear strain was estimated for each sample by either interpolation or extrapolation, where the void ratio in Table 2 was also used and regarded as e_0 in the equation of the ultimate volumetric strain.

The volumes of erupted soil are plotted versus the estimated critical shear strain in Figure 11. Since the relationship for the MX sample was not acquired in Figure 10, all the results except those for the MX sample are shown in Figure 11. The estimated critical shear strain of the Q50 sample was equal to the value shown in Figure 10 because of a lack in the estimation curve for the Q50 sample there. As explained in Figure 11, the result for the Q30 was differed significantly from the other results because of drainage. It is highly likely that the small erupted volume for the Q10 can also be attributed to drainage. However, in general, a denser specimen with lower contraction potential, as shown in Figure 10, tends to result in the eruption of smaller quantities of soil. With this in mind, it would appear reasonable to assume that there is a relation, such as that shown by hatching in Figure 11.

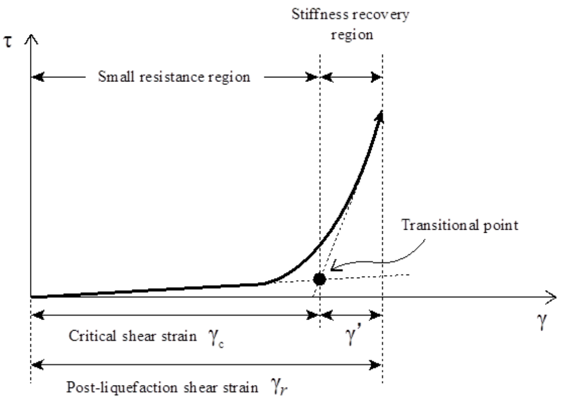

Figure 9. Schematic illustration of the critical shear strain.

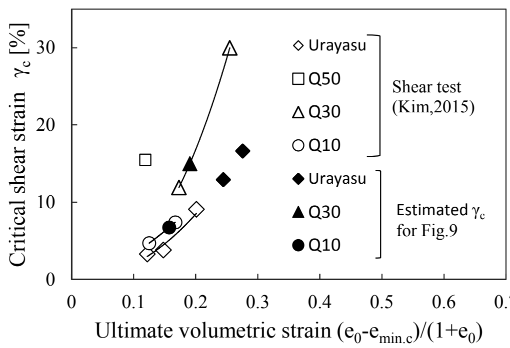

Figure 10. The relationships between the ultimate volumetric strain and the critical shear strain.

Table 3. Cyclic minimum void ratios shown by Kim et al.(2015).

	Urayasu	*MX*	*Q50*	*Q30*	*Q10*
$e_{min,c}$	0.649	none	0.456	0.287	0.52

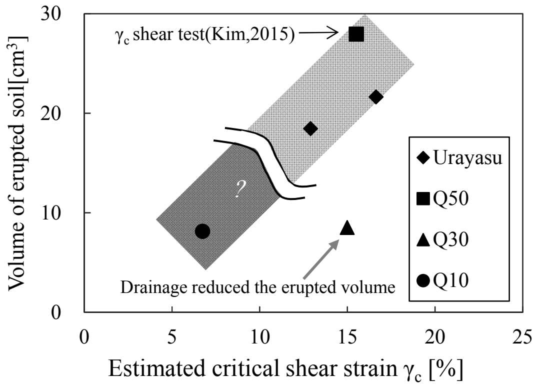

Figure 11. The relation between the critical shear strain and the erupted volume.

5 CONCLUSIONS

The aim of this investigation was to confirm whether it was possible for Type B sand boiling to occur in-situ. That is, with lower permeability and an extremely small shear modulus remaining even after a large amount of deformation, a large amount of shearing occurs and the soil skeleton is squeezed out through the defects in the upper soil layer before drainage recovers the effective stress and the rigidity of the soil skeleton. It is acknowledged that the erupted volumes obtained in this investigation were sensitive to many conditions and in order to estimate the settlement based on this issue the volume should be divided by the area representing the sand boiling. Although these points render the values of the erupted volume obtained in this paper meaningless, the following conclusions were nevertheless confirmed:

a)Type B sand boiling in Figure 1, which is based on squeezing of the liquefied sand by the overburden and where the liquefied soil is highly deformed, does actually happen in reality.

b)It is only possible for this type of sand boiling to occur for a limited type of soils: those with very low permeability and high contraction potential.

c)The erupted volumes of sand boiling appears to be related to the magnitude of the critical shear strain as well as the geometric conditions of the liquefied layer and its flow path up to the ground surface through the upper non-liquefied layer.

REFERENCES

Ishihara K., and Yoshimine M. 1992. Evaluating of settlements in sand deposits following liquefaction during earthquakes,. *Soils and Foundations*, 32(1), 173-188.

Kim J. 2015. *Deformation properties of liquefied soils with fines, PhD Thesis*. Tohoku University.

Miyata M., Iai S. and Ichii K. 1998. Estimation of Differential Settlements due to Liquefaction. *Technical note of the port and harbour research institute ministry of transport 908*. (Japanese)

Sera R., Koike Y. Kuwano R. and Kuwano J. 2014. Sub-surface cavities in the liquefied ground caused by the Great East Japan Earthquake. *Japanese Geotechnical J.*, 9(3), 323-339. (Japanese)

Yasuda, S., Yoshida, N., Adachi, K., Kiku, H., Gose, S. and Masuda, T. (1999): A simplified practical method for evaluating liquefaction-induced flow, *Doboku Gakkai Ronbunshu*, 1999(638), 71-89. (Japanese)